Electronic Supplementary Material (ESI) for Journal of Materials Chemistry A.

Supporting Information

Unveiling $BiVO_4$ Nanorods as a Novel Anode Material for High Performance Lithium Ion Capacitor: Beyond Intercalation Strategy

Deepak P. Dubal,[a, b] Kolleboyina Jayaramulu,[c,d] Radek Zboril,[d] Roland A. Fischer,[c] Pedro Gomez-Romero [b]**

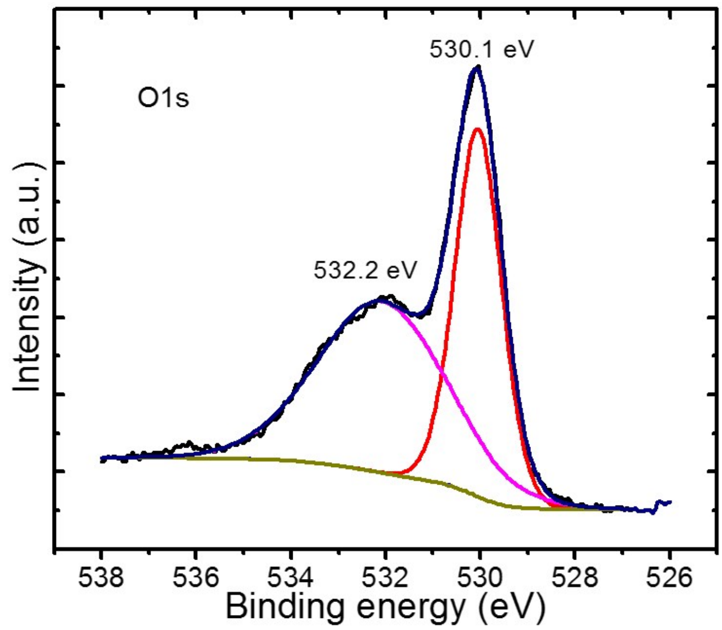

Figure S1 Magnified XPS spectrum for O1s of $BiVO_4$ nanorods with deconvulated peaks.

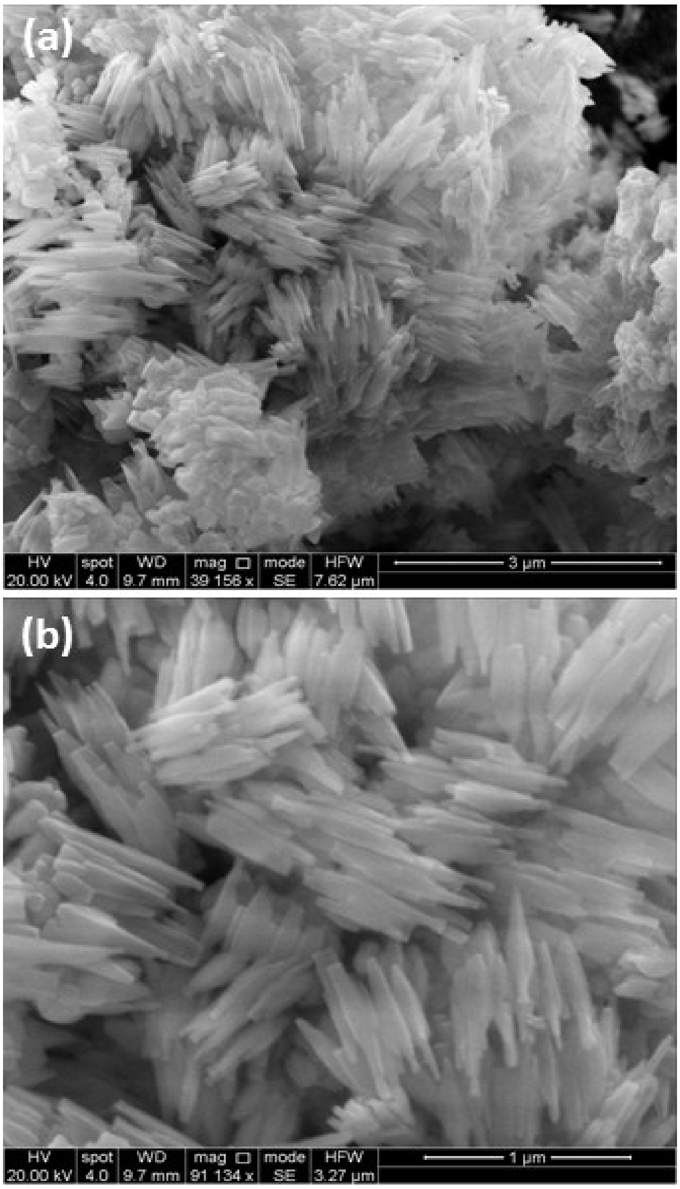

Figure S2 SEM images of $BiVO_4$ nanorods at two different magnifications.

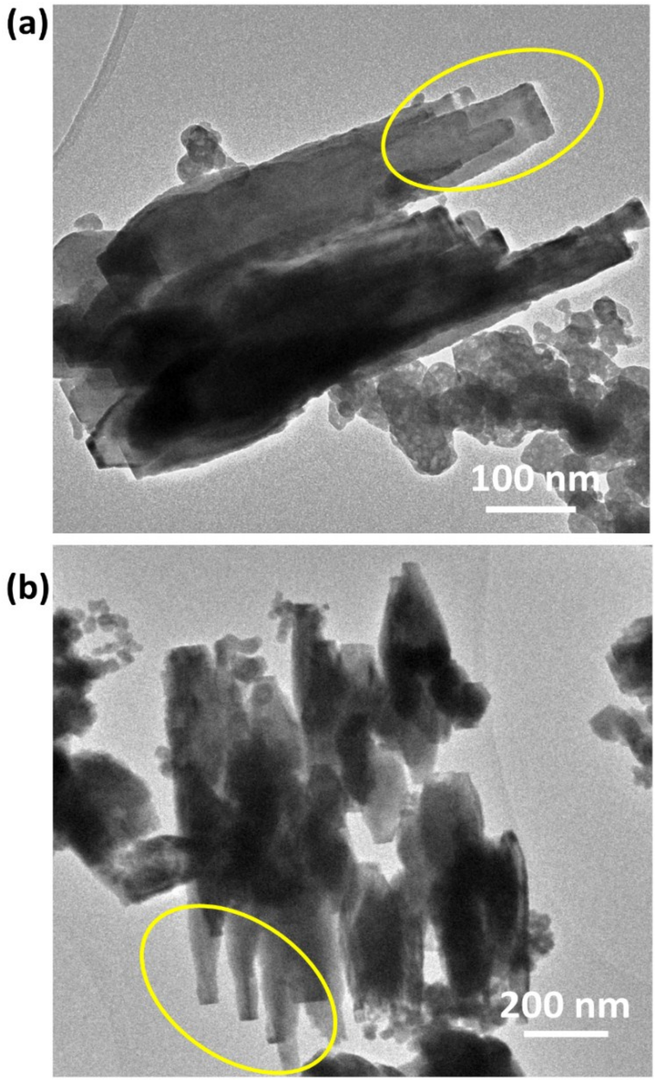

Figure S3 TEM images of $BiVO_4$ nanorods at two different magnifications, suggesting the formation of nanorods.

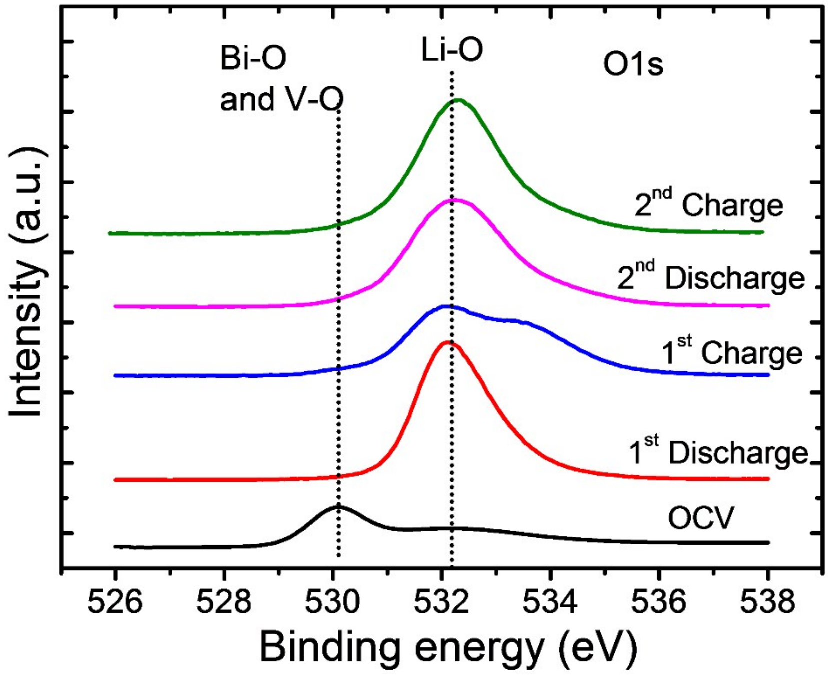

Figure S4 Ex-situ XPS analysis: core-level O1s spectra of $BiVO_4$ electrode after charge/discharge cycles, suggesting the presence of Bi-O, V-O and Li-O.

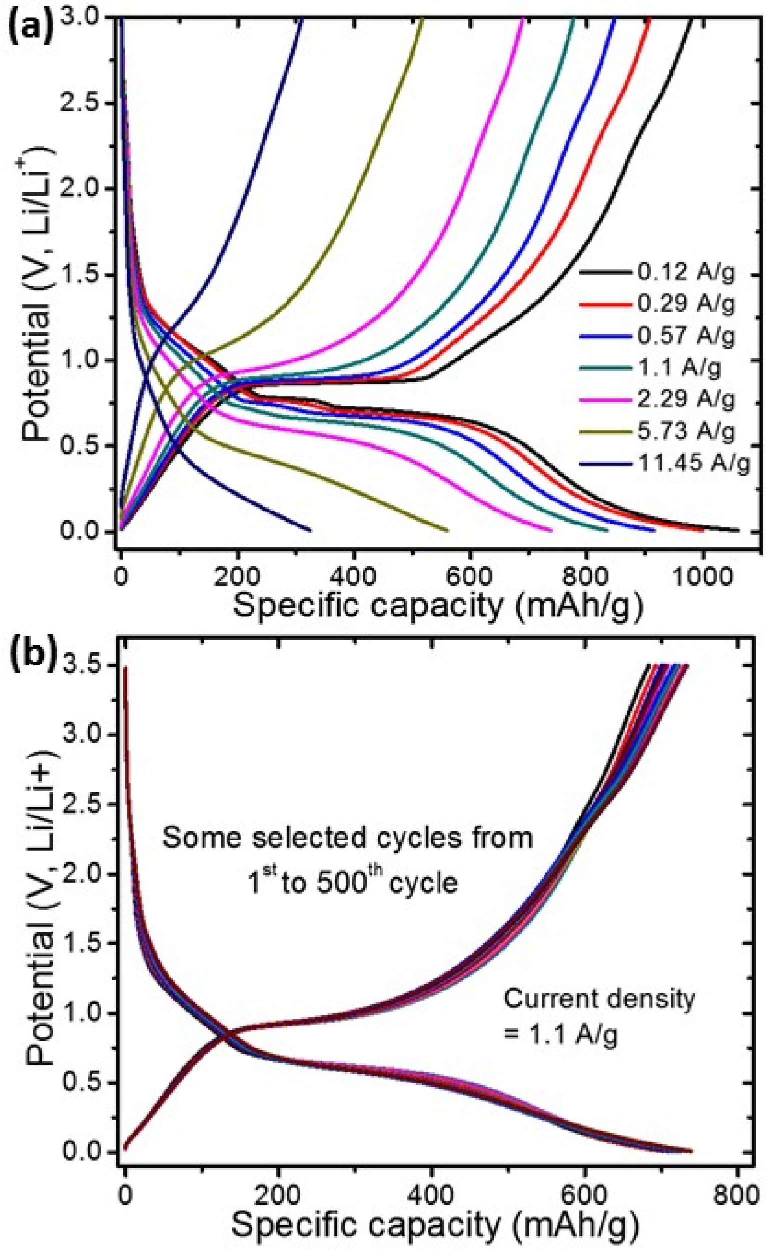

Figure S5 (a) Galvanostatic charge/discharge curves for $BiVO_4$ nanorods in half-cell configuration at different current densities, (b) Few galvanostatic charge/discharge cycles from 500 cycles measured at 1.1 A/g

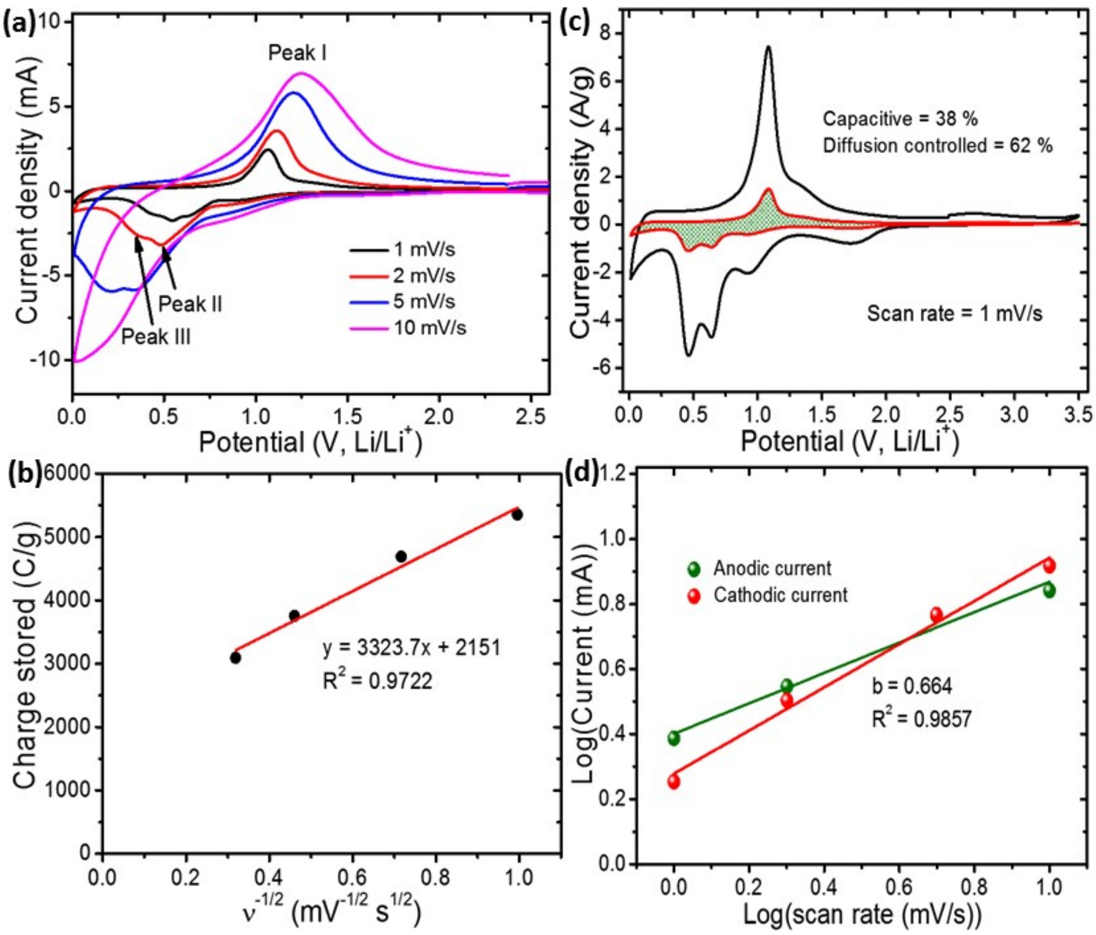

Figure S6 (a) Cyclic voltammetry curves for $BiVO_4$ anode at different scan rates, (b) The plot of total gravimetric charge against the reciprocal of the square root of potential scan rate for $BiVO_4$ electrodes, (c) Voltammetric response at a scan rate of 1 mV/s, the capacitive contribution to the total current is shown by the shaded region, (d) Plot of log (current) vs log(scan rate) for anodic and cathodic responses.

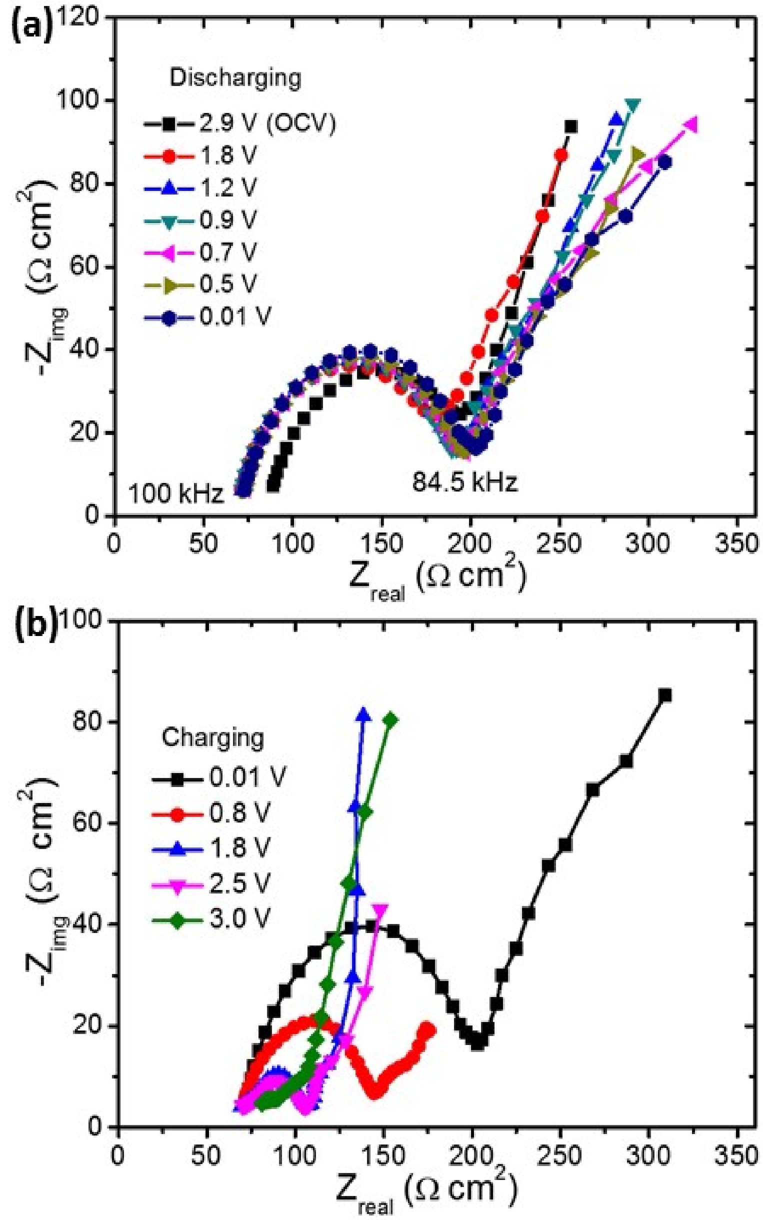

Figure S7 Nyquist plots for $BiVO_4$ anode at differetnt discharging (a) and charging (a) potentials.

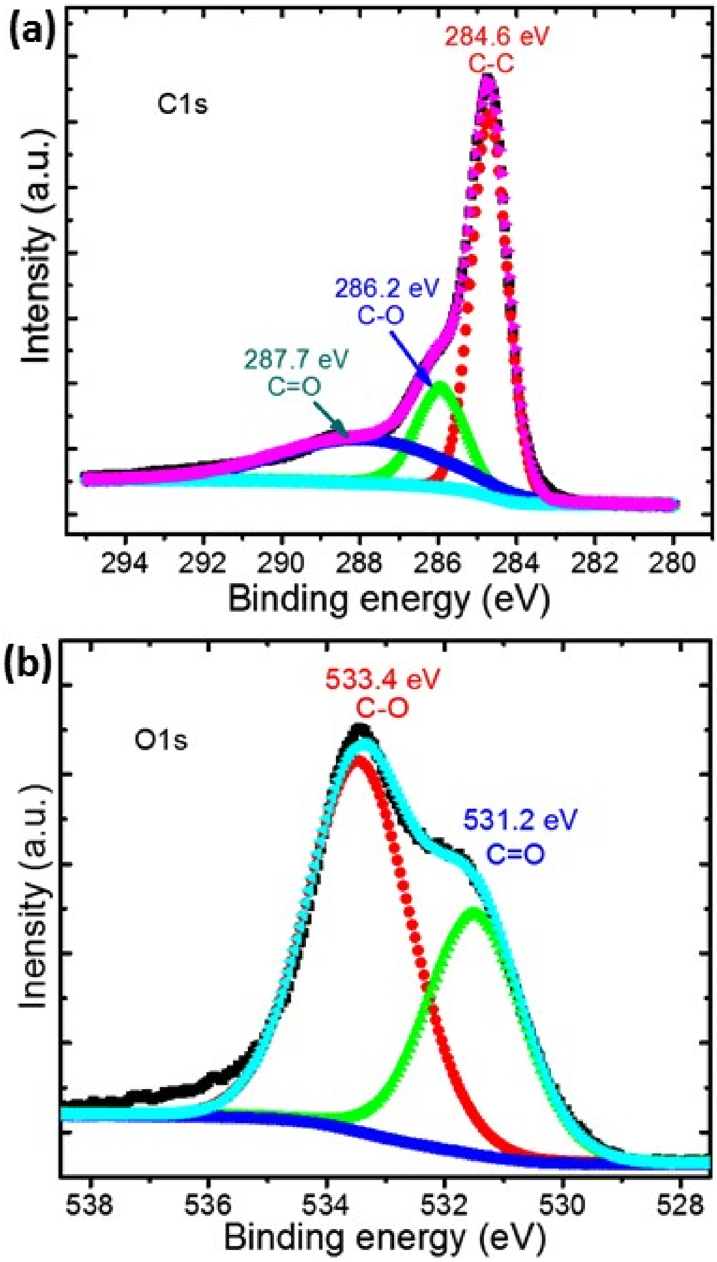

Figure S8 Core-level XPS spectra for (a) C1s and (b) O1s of partially reduced graphene oxide (PRGO) with corresponding deconvulated peaks.

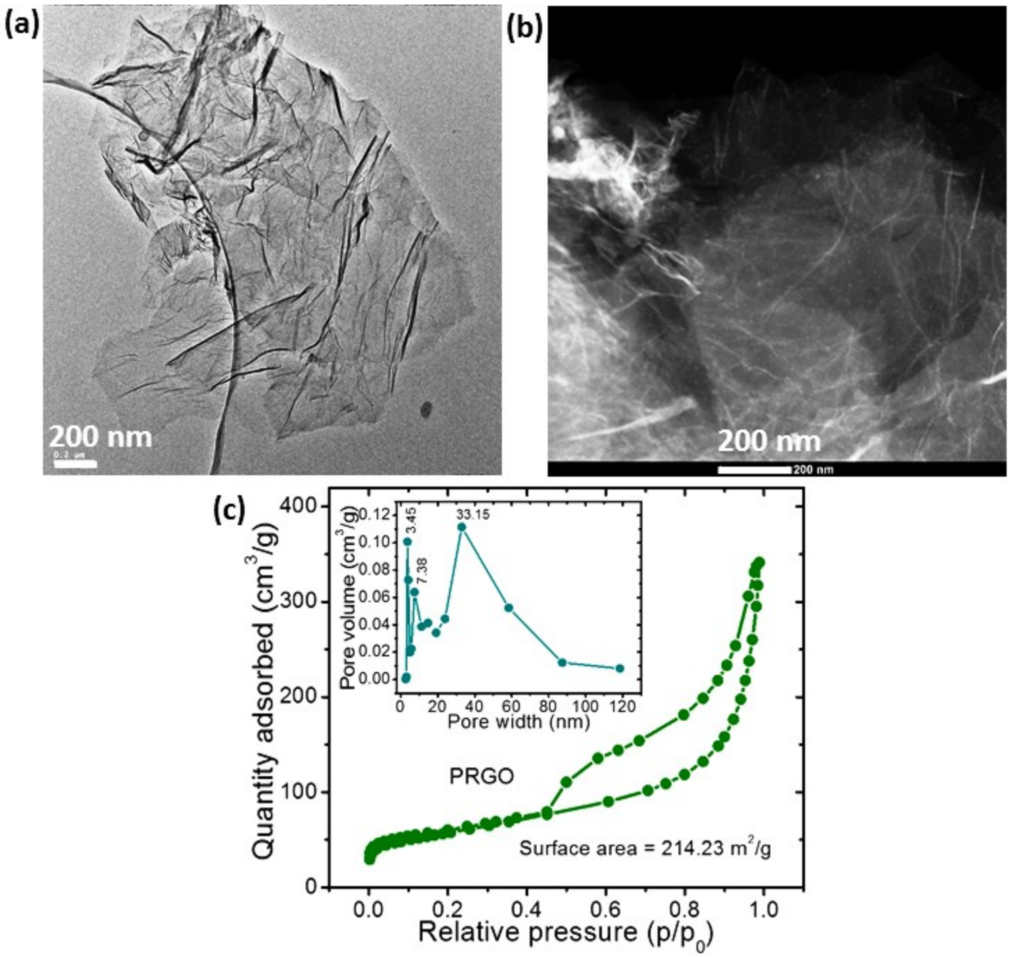

Figure S9 (a) SEM and (b) STEM images of PRGO suggesting the formation of open-porous nanosheets, (c) Nitrogen adsorption/desorption isotherm of PRGO samples with corresponding pore size distribution curves (inset)

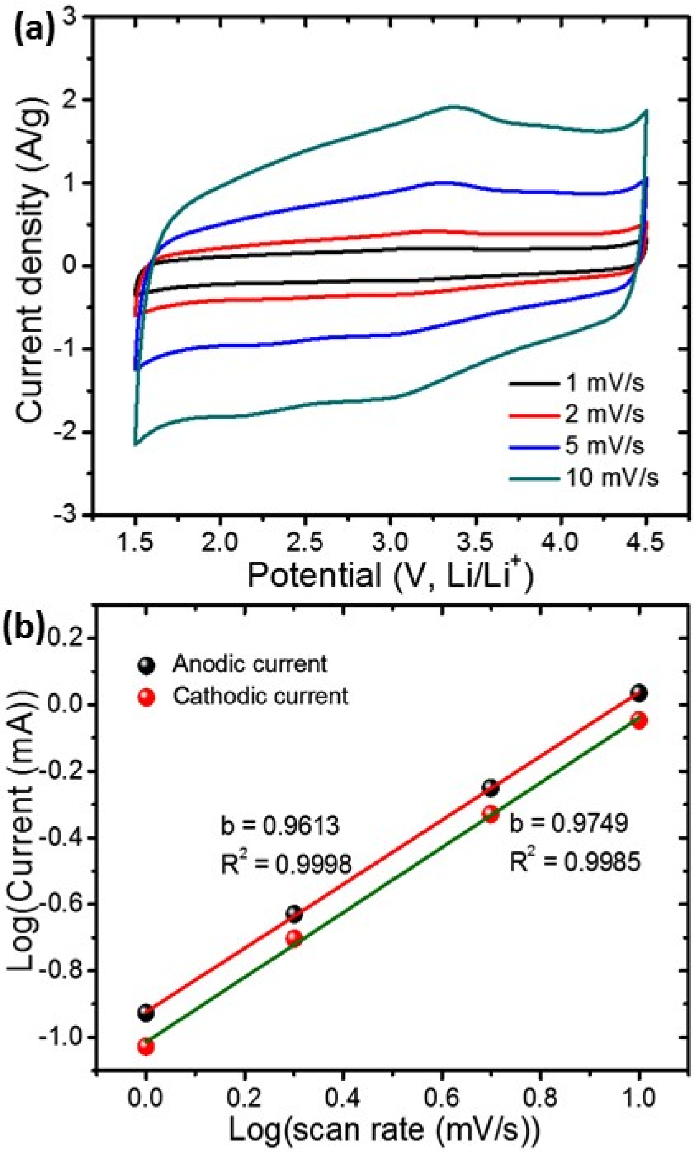

Figure S10 (a) Cyclic voltammetry curves for PRGO cathode at different scan rates (b) Plots of Log(current) vs Log(scan rate) suggesting the major contribution from suface capacitive processes as b ≈ 0.97.

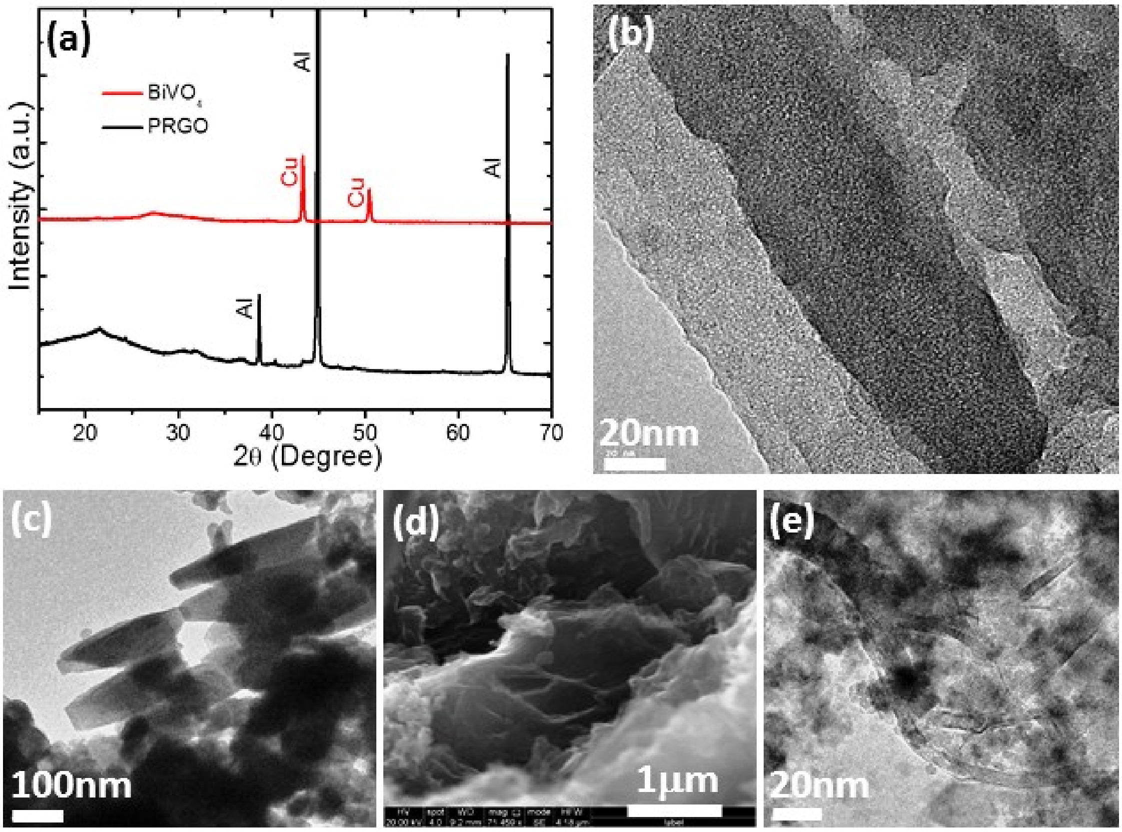

Figure S11 (a) XRD patterns of $BiVO_4$ and PRGO after 6000 cycles, suggesting amorphous nature of the materials. (b and c) TEM images of $BiVO_4$ after 6000 cycles, indicating that $BiVO_4$ still preserves their nanorods-like morphology. (d and e) SEM and TEM image of PRGO after 6000 cycles, respectively. The images suggests that the PRGO maintained their nanosheets-like structure after charge/discharge cycles.

Table S1 Comparison of electrochemical properties of carbon based anode materials with present report

Anode Material	Reversible capacity (mAh/g)	Capacity retention (mAh/g)	References
$BiVO_4$	1035 at 0.12 A/g (5382 mAh/cm^3)	793 at 1.1 A/g after 500 cycles	Present work
$FeVO_4$	1237 at 0.5 A/g (4490 mAh/cm^3)	1237 at 0.5 A/g after 100 cycles	[1]
$FeVO_4$	527 at 0.075 A/g	432 at 0.075 after 100 cycles	[2]
$FeVO_4$-graphene	1046 at 0.1 A/g	1046 at 0.1 A/g after 100 cycles	[3]
Li_3VO_4	323 at 0.02 A/g	283 at 0.02 A/g after 25 cycles	[4]
Li_3VO_4/ N-doped graphene	491 at 0.1 A/g	195 at 2 A/g after 900 cycles	[5]
$Li_3VO_{4-\delta}$	416 at 0.2 A/g	286 at 0.2 A/g after 200 cycles	[6]
Li_3VO_4	422 at 0.394 A/g	376 at 0.394 after 75 cycles	[7]
Li_3VO_4/C/CNTs	397 at 0.394 A/g	272 at 4 A/g after 500 cycles	[8]
Hollow-Cuboid Li_3VO_4/C	415 at 0.2 A/g	415 at 0.2 A/g after 50 cycles 92 % retention after 1000 cycles (10 C = 4 A/g)	[9]
Oxygen deficient Li_3VO_4	495 at 0.1 A/g	270 at 1 A/g after 500 cycles	[10]
Li_3VO_4/C/rGO	435 at 0.4 A/g	325 at 4 A/g (10 C) after 5000 cycles (82.5 % retention)	[11]
Li_3VO_4/rGO	486 at 0.4 A/g	163 at 2 A/g after 5000 cycles (63.1 % retention)	[12]
Carbon-Encapsulated Li_3VO_4	410 at 0.4 A/g	80 % capacity retention after 2000 cycles	[13]
Li_3VO_4	481 at 0.1 A/g	398 at 0.1 A/g after 100 cycles	[14]
Li_3VO_4/C hollow spheres	429 at 0.08 A/g	275 at 4 A/g after 3000 cycles (97 % retention)	[15]
Ce doped $FeVO_4$	1339 at 0.09 A/g	513 at 0.09 A/g after 40 cycles	[16]

Table S2 Comparison of published electrochemical properties of Li-ion capacitors with our present work

LIC cell	Energy density (Wh/kg)	Power density (W/kg)	Voltage (V)	Cycling stability	References
$BiVO_4$//PRGO	152 at 384 W/kg	3861 at 42 Wh/kg	4.0	79 % after 4000 cycles	Present work
$Li_4Ti_5O_{12}$//AC[2]	67.5 at 490 W/kg	4995 at 33.6 Wh/kg	3.0	85 % after 2000 cycles	[17]
Graphene//FRGO[3]	148.3 at 141 W/kg	7800 at 71.5 Wh/kg	4.2	68 % after 3000 cycles	[18]
Graphene-$Li_4Ti_5O_{12}$// Graphene/Sucrose	95 at 40 W/kg	3000 at 32 Wh/kg	3.0	87 % after 500 cycles	[19]
Li_3VO_4//AC	49.1 at 72.5 W/kg	129.7 at 24.5 Wh/kg	3.5	-	[20]
$LiTi_{1.5}Zr_{0.5}(PO_4)_3$// AC	46.7 at 79.2 W/kg	8120 at 9.91 Wh/kg	3.4	93 % after 100 cycles	[21]
Fe_3O_4-Graphene// 3D Graphene	147 at 150 W/kg	2587 at 86 Wh/kg	3.0	70 % after 1000 cycles	[22]
TiC//PHPNC[4]	112 at 450 W/kg	67500 at 35.6 Wh/kg	4.5	83%, 5000 cycles	[23]
Graphene-VN //carbon nanorods	162 at 200 W/kg	10000 at 64 Wh/kg	4.0	86%, 1000 cycles	[24]
CNT/V_2O_5//AC	25.5 at 40 W/kg	6300 at 6.9 Wh/kg	2.7	80%, 10000 cycles	[25]
TiO_2-B nanowire//CNT	12.5 at 300 W/kg	1300 at 8 Wh/kg	2.8	1000 cycles	[26]
TiP_2O_7//AC	13 at 46 W/kg	370 at 0.2 Wh/kg	3.0	78%, 500 cycles	[27]
Li-Hard carbon//AC	82 at 100 W/kg	50000 at 1 Wh/kg	2.8	100 % after 40 cycles	[28]

[1]FGO-functionalized graphene oxide, [2]AC-activated carbon, [3]FRGO-flash reduced graphene oxide, [4]PHPNC- pyridine-derived hierarchical porous nitrogen-doped carbon

References

[1] D. H. Sim, X. Rui, J. Chen, H. Tan, T. M. Lim, R. Yazami, H. H. Hng, Q. Yan, Direct growth of $FeVO_4$ nanosheet arrays on stainless steel foil as high-performance binder-free Li ion battery anode, *RSC Advances*, **2012**, 2, 3630-3633

[2] N. Yan, Y. Xu, H. Li, W. Chen, The preparation of $FeVO_4$ as a new sort of anode material for lithium ion batteries, *Mater. Lett.* **2016**, 165, 223-226

[3] X. Liu, Y. Cao, H. Zheng, X. Chen, C. Feng, Synthesis and modification of $FeVO_4$ as novel anode for lithium-ion batteries, *Appl. Surf. Sci.* **2017**, 394, 183-189

[4] H. Li, X. Liu, T. Zhai, D. Li, H. Zhou, Li_3VO_4: A Promising Insertion Anode Material for Lithium-Ion Batteries, *Adv. Energy Mater.* **2013**, *3*, 428-432

[5] S. Ni, J. Zhang, J. Ma, X. Yang, L. Zhang, Li_3VO_4/N-doped graphene with high capacity and excellent cycle stability as anode for lithium ion batteries, *J. Power Sources* **2015**, 296, 377-382

[6] L. Chen, X. Jiang, N. Wang, J. Yue, Y. Qian, J. Yang, Surface-Amorphous and Oxygen-Deficient $Li_3VO_{4-\delta}$ as a Promising Anode Material for Lithium-Ion Batteries, *Adv. Sci.* **2015**, *2*, 1500090

[7] L. L. Zhou, S. Y. Shen, X. Peng, L. N. Wu, Q. Wang, C. H. Shen, T. T. Tu, L. Huang, J. T. Li, S. G. Sun, New insights into the structure changes and interface properties of Li_3VO_4 anode for lithium ion batteries during the initial cycle by in-situ techniques, *ACS Appl. Mater. Interfaces*, **2016**, *8*, 23739-23745

[8] Y. Yang, J. Li, D. Chen, J. Zhao, Spray Drying-Assisted Synthesis of Li_3VO_4/C/CNTs Composites for High-Performance Lithium Ion Battery Anodes, *J. Electrochem. Soc.* **2017**, 164, A6001-A6006

[9] C. Zhang, C. Liu, X. Nan, H. Song, Y. Liu, C. Zhang, G. Cao, Hollow-cuboid Li_3VO_4/C as High Performance Anodes for Lithium-Ion Batteries, *ACS Appl. Mater. Interfaces*, **2016**, *8*, 680-688

[10] K. Wang, C. Zhang, H. Fu, C. Liu, Z. Lia, W. Ma, X. Lu, G. Cao, Enhanced electrochemical properties of Li_3VO_4 with controlled oxygen vacancies as Li-ion battery anode, *Chem. Eur. J.* **2017**, 10.1002/chem.201700150

[11] Q. Li, Q. Wei, J. Sheng, M. Yan, L. Zhou, W. Luo, R. Sun, L. Mai, Mesoporous Li_3VO_4/C Submicron-Ellipsoids Supported on Reduced Graphene Oxide as Practical Anode for High Power Lithium-Ion Batteries, *Adv. Sci.* **2015**, 1500284

[12] Z. Jian, M. Zheng, Y. Liang, X. Zhang, S. Gheytani, Y. Lan, Y. Shi, Y. Yao, Li_3VO_4 anchored graphene nanosheets for long-life and high-rate lithium-ion batteries, *Chem. Commun.*, **2015**, 51, 229-231

[13] C. Zhang, H. Song, C. Liu, Y. Liu, C. Zhang, X. Nan, G. Cao, Fast and Reversible Li Ion Insertion in Carbon-Encapsulated Li_3VO_4 as Anode for Lithium-Ion Battery, *Adv. Funct. Mater.*

2015, 25, 3497–3504

[14] S. Ni, X. Lv, J. Ma, X. Yang, L. Zhang, Electrochemical characteristics of lithium vanadate, Li_3VO_4 as a new sort of anode material for Li-ion batteries, *J. Power Sources* **2014**, 248, 122-129

[15] Y. Yang, J. Li, X. He, J. Wang, D. Sun, J. Zhao, Facile spray drying route for mesoporous Li_3VO_4/C hollow spheres as an anode for long life lithium ion batteries, *J. Mater. Chem. A*, **2016**, 4, 7165-7168

[16] M. Y. Shad, M. Nouri, A. Salmasifar, H. Sameie, R. Salimi, H. Eivaz Mohammadloo, A. A. Sabbagh Alvani, M. Ashuri, M. Tahriri, Wet-Chemical Synthesis and Electrochemical Properties of Ce-Doped $FeVO_4$ for Use as New Anode Material in Li-ion Batteries, *J. Inorg. Organomet. Polym.* **2013**, 23, 1226

[17] Jain, A. et al., Activated carbons derived from coconut shells as high energy density cathode material for Li-ion capacitors, *Sci. Rep.* **3**, 3002 (2013)

[18] Zhang, T. et al., High energy density Li-ion capacitor assembled with all graphene-based electrodes, *Carbon* **92**, 106-118 (2015).

[19] Leng, K. et al., Graphene-based Li-ion hybrid supercapacitors with ultrahigh performance, *Nano Res.* **6**, 581-592 (2013).

[20] Wei, H. Y., Tsai, D. S., Hsieh, C. L., Prelithiated lithium vanadate anode and the mass balancing of its hybrid capacitor, *RSC Adv.*, **5**, 69176-69183 (2015)

[21] Peng, C. J., Tsai, D. S., Chang, C., Wei, H. Y., The lithium ion capacitor with a negative electrode of lithium titanium zirconium phosphate, *J. Power Sources* **274**, 15-21 (2015)

[22] Zhang, F. et al., A high-performance supercapacitor-battery hybrid energy storage device based on graphene-enhanced electrode materials with ultrahigh energy density, *Energy Environ. Sci.*, **6**, 1623-1632 (2013)

[23] Wang, H.; et al. A high-energy lithium-ion capacitor by integration of a 3D interconnected titanium carbide nanoparticle chain anode with a pyridine-derived porous nitrogen-doped carbon cathode, *Adv. Funct. Mater.***26**, 3082-3093 (2016)

[24] Wang, R., Lang, J., Zhang, P., Lin, Z., Yan, X., Fast and Large Lithium Storage in 3D Porous VN Nanowires–Graphene Composite as a Superior Anode Toward High-Performance Hybrid Supercapacitors, *Adv. Funct. Mater*. **25**, 2270-2278 (2015)

[25] Chen, Z. et al., High-Performance Supercapacitors Based on Intertwined CNT/V_2O_5 Nanowire Nanocomposites, *Adv. Mater.* **23**, 791-795 (2011)

[26] Wang, Q., Wen, Z., Li, J., A Hybrid Supercapacitor Fabricated with a Carbon Nanotube Cathode and a TiO_2–B Nanowire Anode, *Adv. Funct. Mater*. **16**, 2141-2146 (2006)

[27] Aravindan, V. et al., Hybrid supercapacitor with nano-TiP_2O_7 as intercalation electrode, *J.*

Power Sources, **196**, 8850-8854 (2011)

[28] Cao, W. J., Zheng, J. P., Li-ion capacitors with carbon cathode and hard carbon/stabilized lithium metal powder anode electrodes, *J. Power Sources* **213**, 180-185 (2012)